

On the metal-insulator transition in n-type doped CuGaSe₂

This article has been downloaded from IOPscience. Please scroll down to see the full text article.

2000 J. Phys.: Condens. Matter 12 4603

(<http://iopscience.iop.org/0953-8984/12/21/305>)

View [the table of contents for this issue](#), or go to the [journal homepage](#) for more

Download details:

IP Address: 171.66.16.221

The article was downloaded on 16/05/2010 at 05:08

Please note that [terms and conditions apply](#).

On the metal–insulator transition in n-type doped CuGaSe₂

J H Schön†, Ch Kloc†, E Arushanov‡, G A Thomas† and E Bucher†§

† Bell Laboratories, Lucent Technologies, 600 Mountain Avenue, Murray Hill, New Jersey, USA

‡ Institute of Applied Physics, Academy of Sciences of Moldova, Kishinev, Moldova

§ Universität Konstanz, Fakultät für Physik, PO Box X916, D-78547 Konstanz, Germany

Received 18 January 2000, in final form 24 March 2000

Abstract. Transport properties of n-type CuGaSe₂ single crystals are investigated in the temperature range from 2 to 350 K. The effective donor concentration is varied between 2×10^{12} and $4.4 \times 10^{17} \text{ cm}^{-3}$ by co-doping with Ge and Zn. The charge transport properties are analysed and interpreted in the framework of an Anderson metal–insulator transition. A critical donor concentration N_c of $1.4 \times 10^{17} \text{ cm}^{-3}$ is estimated, which is in good agreement with the Mott criterion ($N_c^{1/3} \approx 0.25/a_H$). However, the second characteristic concentration, above which the Fermi level merges into the conduction band, was not observed experimentally. This is in accordance with an estimate of $7 \times 10^{17} \text{ cm}^{-3}$ according to the Matsubara–Toyozawa criterion, which exceeds the highest donor concentrations achieved in this material so far. The effective dopant density in n-type CuGaSe₂ is limited by self-compensation due to intrinsic defects (mainly Cu vacancies). Furthermore, at low temperatures a crossover from Mott- to Efros–Shklovskii-type variable range hopping is observed on the dielectric side of the transition.

1. Introduction

CuGaSe₂ (CGS), belonging to the I–III–VI₂ family of chalcopyrite compounds, has been studied as a promising material for photovoltaic applications. Because its energy gap of 1.72 eV is well suited for the solar spectrum, efficiencies exceeding 9% have been obtained for single crystal as well as thin film solar cells [1, 2]. Recently, it has been demonstrated that n-type CGS can be achieved by co-doping with Ge and Zn [3]. The samples have been doped with Ge by ion implantation and post-treated in a Zn atmosphere. Room temperature carrier concentrations of 10^{16} cm^{-3} have been reported. Here we show that the carrier concentration at room temperature can be increased significantly by optimizing the post-deposition annealing parameters. Electron densities at room temperature as high as $4.4 \times 10^{17} \text{ cm}^{-3}$ are achieved. It was previously shown that at high donor concentrations an impurity band is formed [4]. In this study we investigated the electronic transport properties of n-CGS single crystals as a function of the effective, uncompensated donor density ($N_d - N_a$).

At low donor concentrations there is a negligible overlap of the hydrogenic wave functions of the donor levels. Hence, the material is insulating. At high concentrations the material becomes a metal, when the overlap is large compared to the on-site electron–electron repulsion. The transition from the insulating to metallic state (i.e., localized to itinerant electrons) occurs at a critical concentration N_c , when the average spacing between the impurities is approximately four times the Bohr radius [5]. This kind of metal–insulator transition (MIT) has also been observed in n-CuInSe₂, a closely related compound [6]. Another view of the MIT, due to Anderson [7], involves localization due to random one-electron potentials seen by the electrons. At low donor densities the energy spread in the random potential of the disordered system is

large compared to the energy bandwidth. As a result of this, the electronic states of the system are localized. At higher concentrations extended states, separated by a mobility edge, are formed. Within the Anderson framework the MIT occurs if the Fermi level E_F is pushed through the mobility edge by the addition of electrons [7, 8]. Mott proposed a discontinuous drop [9] of the zero-temperature electrical conductivity at N_c , whereas scaling theories of localization suggest a continuous decrease [8, 10] as the donor concentration is lowered to N_c . The experimental results for n-CGS will be discussed in the framework of an Anderson MIT.

2. Experimental methods

CGS single crystals were grown by chemical vapour transport using iodine as transport agent. Some crystals were doped during CVT growth with Ge and Zn, resulting in highly resistive n-type material. Ge-ion implantation was carried out using an energy of 150 keV and a dose of $5 \times 10^{15} \text{ cm}^{-2}$ on undoped CGS crystals [3]. Annealing in the presence of Zn was carried out in a flow of hydrogen for 24 h at temperatures up to 500 °C. Resistivity and Hall-effect measurements (magnetic field up to 2 T) were carried out in the temperature range from 2 to 350 K using a conventional DC set-up. Furthermore, magnetoresistance at low temperatures has been studied in these samples using magnetic fields up to 8 T. Ohmic contacts to n-CGS samples were prepared using thermal evaporation of In.

3. Results and discussion

Co-doping with Ge and Zn provides a means to obtain n-type CGS crystals [3]. Resistivity ρ and Hall coefficient R_h of the various samples are shown in figures 1 and 2 as functions of

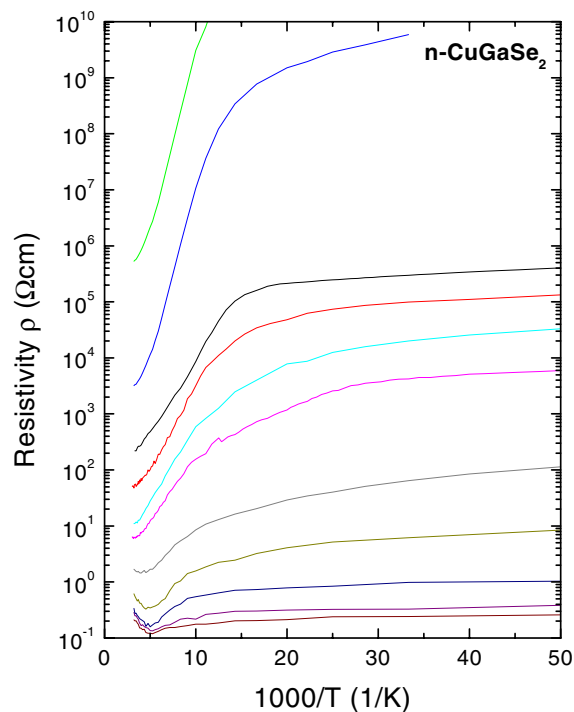


Figure 1. Resistivity of doped n-type CuGaSe₂ single crystals as a function of reciprocal temperature (sample 1 (top curve) to sample 11 (bottom curve)).

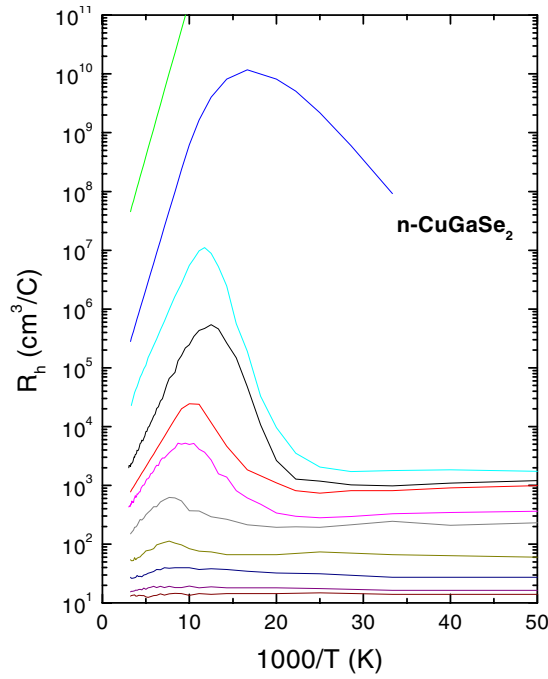


Figure 2. Hall coefficient of doped n-type CuGaSe₂ single crystals as a function of reciprocal temperature (sample 1 (top curve) to sample 11 (bottom curve)).

temperature. The electron mobility in these samples is in the range of $100 \text{ cm}^2 \text{ V}^{-1} \text{ s}^{-1}$ at room temperature and reaches maximum values up to $500 \text{ cm}^2 \text{ V}^{-1} \text{ s}^{-1}$ at low temperatures. The donor and acceptor concentrations N_d and N_a , the activation energy E_d and the degree of compensation $K = N_a/N_d$ can be estimated from the Hall coefficient R_h [3,4]. The effective donor concentration ($N_d - N_a$) can be estimated in the carrier freezing region and the degree of compensation can be extracted from the temperature dependence of the Fermi energy assuming a one donor and one acceptor model [4]. The obtained values are summarized in table 1. The effective donor concentration ($N_d - N_a$) depends significantly on the preparation of the samples. Whereas CVT growth generally results in heavy compensation ($K \approx 1$), additional annealing in the presence of Zn reduces the degree of compensation. We assume that spontaneous formation of Cu vacancies (V_{Cu}) causes strong self-compensation as the Fermi level shifts to the conduction band [11–13]. This is minimized in the presence of Zn due to the formation of Zn_{Cu} defects, which act as additional donors in contrast to compensating V_{Cu} acceptor levels. At too high Zn-annealing temperatures the degree of compensation increases again (see table 1), which might be ascribed to the formation of Zn_{Ga} acceptor defects [14]. Furthermore, Ge doping becomes more effective due to an increase of Ge_{Ga} levels compared to Ge_{Cu} defects [3]. We believe that Ge_{Ga} forms a much more shallow level in CGS than Ge_{Cu} . However, a detailed microscopic understanding of self-compensation and co-doping in CGS is still missing.

In order to analyse the temperature dependence of the resistivity we used the reduced activation energy w , given by [15]

$$w = \frac{E}{kT} = \frac{1}{T} \frac{d \ln \rho}{d T^{-1}}. \quad (1)$$

Table 1. Summary of the electrical properties (effective donor concentration $N_d - N_a$, characteristic Mott hopping temperature T_0 , donor activation energy E_d , compensation ratio $K = N_a/N_d$, localization length ξ) of the various n-CuGaSe₂ samples studied. The samples were doped during the chemical vapour transport growth (CVT) or by a subsequent ion-implantation step (Im). The numbers in the second column correspond to the Zn-annealing temperature in °C.

Sample	Growth parameters	$N_d - N_a$ (cm ⁻³)	T_0 (K)	E_d (meV)	K	ξ (nm)
1	CVT	2×10^{12}	—	99	0.99996	
2	CVT/350	3×10^{14}	35 000	102	0.998	7.4
3	CVT/400	3.6×10^{15}	29 000	86	0.95	7.9
4	Im/350	6.4×10^{15}	22 000	79	0.89	8.6
5	CVT/500	7.9×10^{15}	15 000	74	0.89	9.9
6	Im/375	1.7×10^{16}	5 500	68	0.93	13.7
7	CVT/450	4.4×10^{16}	580	49	0.54	29.4
8	Im/400	1.2×10^{17}	3	23	0.81	165
9	Im/425	2.2×10^{17}	—	4	0.64	
10	Im/475	3.5×10^{17}	—	—	0.27	
11	Im/450	4.4×10^{17}	—	—	0.41	

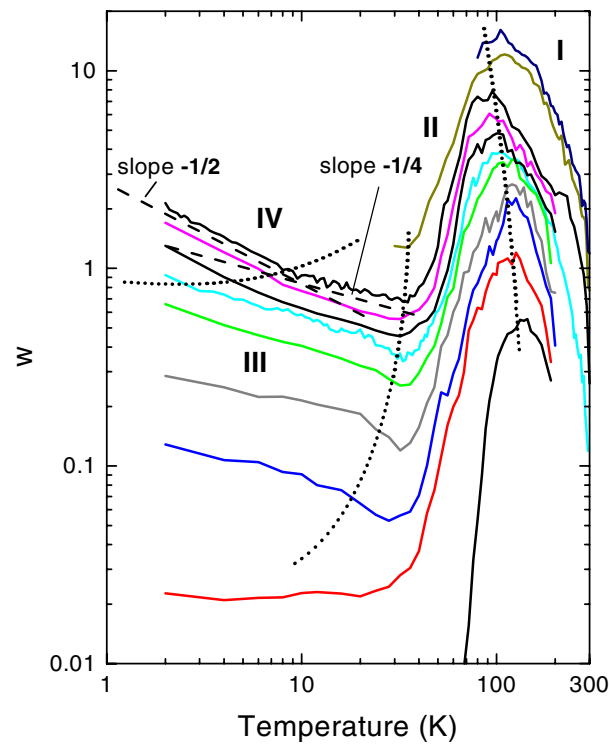


Figure 3. Reduced activation energy w of doped n-type CuGaSe₂ single crystals as a function of temperature (sample 1 (top curve) to sample 11 (bottom curve)). The different regions (I–IV) are described in the text. The dashed lines correspond to a slope of $-1/2$ (Efros–Shklovski variable range hopping) and $-1/4$ (Mott variable range hopping).

By plotting $\log w$ against $\log T$ it is possible to identify the different regions of charge transport (see figure 3). Over the whole temperature range we can discern two (I, III)

characteristic regions with different temperature dependences separated by a transition region (II). At low temperatures the transport is governed by tunnelling and hopping. The electrical conductivity occurs by electronic excitations in the vicinity of the Fermi level. The charge transport (except for the two samples with the highest carrier concentration) can be described by Mott-type variable range hopping [16]:

$$\rho(T) = \rho_0 \exp\left(\frac{T_0}{T}\right)^{1/4}. \quad (2)$$

In some samples we observe a crossover from Mott-type to Efros–Shklovskii-type variable range hopping (region IV), where the resistivity is given by [17]:

$$\rho(T) = \rho_{ES} \exp\left(\frac{T_{ES}}{T}\right)^{1/2}. \quad (3)$$

Efros–Shklovskii hopping is expected in the presence of a parabolic ‘Coulomb gap’. If the thermal hopping energy becomes large compared to the energy width of the gap a crossover to Mott-type variable range hopping can be observed [18]. A detailed study of the crossover and the ‘weakening’ of the ‘Coulomb gap’ due to finite temperature effects will be reported elsewhere [19]. The different hopping regimes can be identified by the different slopes in the plot of $\log w$ against $\log T$ (figure 3), $-\frac{1}{2}$ for Shklovskii–Efros and $-\frac{1}{4}$ for Mott-type hopping, respectively.

The characteristic hopping temperatures T_0 and T_{ES} are obtained from a fit of the experimental data to equations (2) and (3), respectively, using a fixed hopping exponent of $\frac{1}{4}$ and $\frac{1}{2}$. The characteristic Mott temperature T_0 allows us to estimate the localization length ξ by [20]

$$\xi = \left(\frac{18}{kT_0 N(E_f)}\right)^{1/3} \quad (4)$$

where $N(E_f)$ is the density of states at the Fermi energy E_f . However, the exact value of $N(E_f)$ is not known. A rough estimation can be obtained using [17, 21]

$$N(E_f) \approx \frac{K N_d}{E_0} \quad (5)$$

where $E_0 = e^2/(4\pi\epsilon_0\epsilon_r r_d)$ is the energy of the Coulomb repulsion and $r_d = (4\pi N_d/3)^{-1/3}$ is half the mean distance between the donors. Similar values of $N(E_f)$ are obtained from the positive magnetoresistance at moderate fields. Hence, we assume that the estimation accords to a reasonable approximation of $N(E_f)$. Using the estimated value for $N(E_f)$ and equation (4) the coherence length can be calculated. The values for ξ are summarized in table 1. Note that ξ is expected to diverge as the MIT is approached from the insulating side. Hence, T_0 should go to zero at the transition, which is observed experimentally (see figure 4). A critical concentration N_c of $1.4 \times 10^{17} \text{ cm}^{-3}$ can be estimated graphically (see figure 4). The value of N_c , which defines the MIT, is given by the Mott criterion [5]

$$N_c \approx (0.25/a_H)^3 \quad (6)$$

where a_H is the Bohr radius of the impurity atom ($a_H = a_0\epsilon_r/m^*$) and a_0 that of hydrogen. Using values of $m^* = 0.11 m_e$ (obtained from Hall- and Seebeck-effect measurements) [22] and $\epsilon_r = 9.6$ [23], a value of $1.5 \times 10^{17} \text{ cm}^{-3}$ can be estimated. On the metallic side of the transition the activated temperature dependence of the resistivity (samples 1–9) changes to a power law behaviour (samples 10, 11) [5]. Furthermore, the low temperature conductivity σ_0 (estimated from the conductivity measured at 2 K) goes to zero for dopant concentrations close

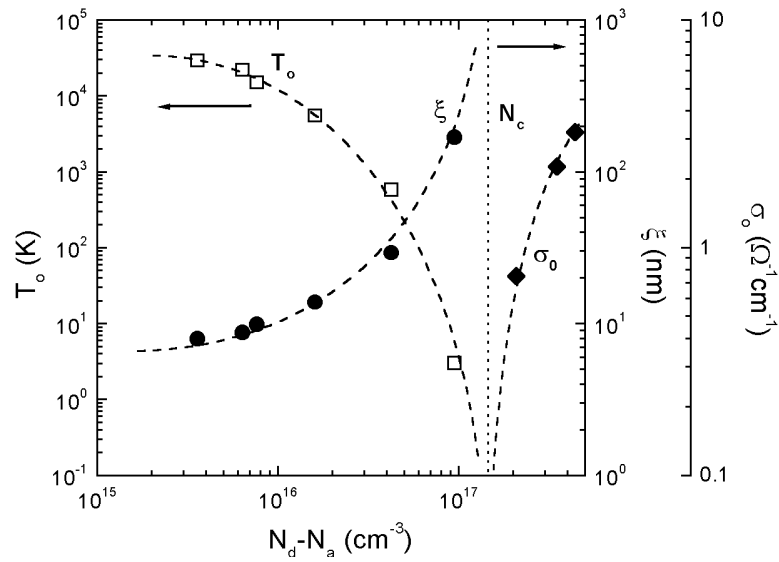


Figure 4. Characteristic Mott temperature T_0 , localization length ξ and low temperature conductivity σ_0 as functions of uncompensated, effective donor concentration $N_d - N_a$. A critical concentration of $1.4 \times 10^{17} \text{ cm}^{-3}$ is estimated graphically (vertical line). The dashed lines are a guide to the eye.

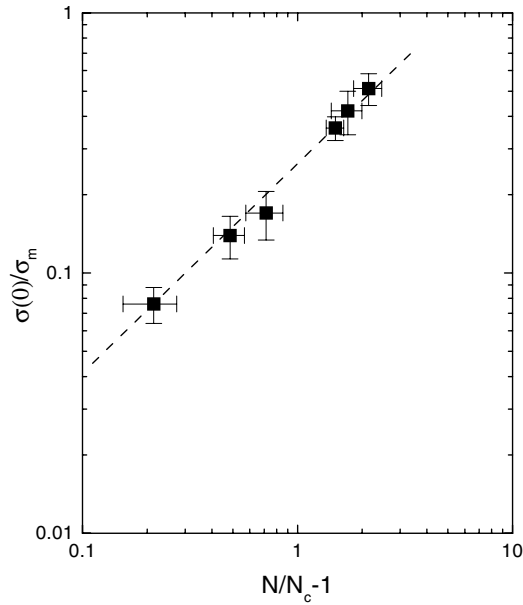


Figure 5. Low temperature conductivity σ_0 as a function of donor concentration $N/N_c - 1$ ($N = N_d - N_a$) for samples on the metallic side of the transition. The dashed line corresponds to a critical exponent of the order of one ($\sigma(0)/\sigma_m \approx (N/N_c - 1)$).

to N_c (see figures 4 and 5). The decrease agrees well with a critical exponent ν of the order of 1 according to scaling theories [10, 24]

$$\sigma(0)/\sigma_m = ((N_d - N_a)/N_c - 1)^\nu \tag{7}$$

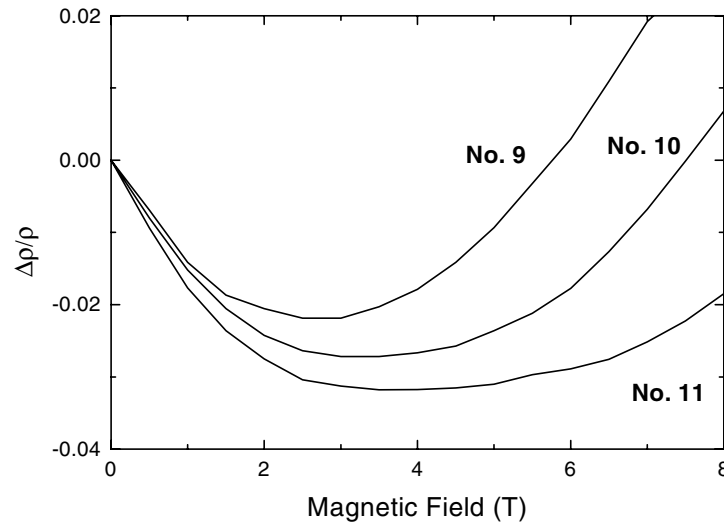


Figure 6. Magnetoconductance of samples 9–11 at 4 K. The minimum shifts to higher magnetic fields as $N_d - N_a$ approaches N_{CB} .

where σ_m is the minimum metallic conductivity ($\sigma_m = 0.05e^2N_c^{1/3}/\hbar$) [9]. It has been pointed out that disorder and compensation broadens the shape of the conductivity– $N/N_c - 1$ curves [24]. This might arise due to a decrease of the relative importance of Coulomb interactions [25] compared to the random potential scattering considered by localization theory [26].

A second characteristic concentration, N_{CB} , above which the Fermi level merges into the conduction band and leads to the metallic conduction, is expressed according to the Matsubara–Toyozawa criterion [27]. N_{CB} can be related to N_c by approximately $N_{CB} \approx 5N_c$ [28]. Hence a value of $7 \times 10^{17} \text{ cm}^{-3}$ can be estimated for N_{CB} , which is higher than the highest doping concentration achieved so far (sample 11). In the intermediate regime ($N_c < (N_d - N_a) < N_{CB}$) the charge transport is governed by a conducting ‘impurity’ band. The magnetoconductance at low temperatures (4 K) exhibits a minimum (see figure 6). This minimum moves to higher magnetic fields with increasing donor concentration. A vanishing of this minimum has been observed in doped Si [28] for concentrations exceeding N_{CB} . This shows that the carrier concentration in n-CGS approaches N_{CB} , but is still smaller than N_{CB} . The positive and negative contributions to the magnetoconductance may arise from orbit shrinkage, Coulomb interaction [29] or localization effects [30]. The magnetoconductance in n-CGS will be the topic of a forthcoming article.

The thermal activation energy of the dominant donor level, which is tentatively ascribed to Ge_{Ga} defects [3], decreases with increasing effective donor concentration (see figure 7). This can be explained by screening effects. Generally, $E_d(N_d - N_a)$ might be described by [31]

$$E_d(N_d - N_a) = E_{d0} - \alpha(N_d - N_a)^{1/3} \quad (8)$$

where E_{d0} is the thermal ionization energy of the donor level in the infinite dilution limit and α a constant describing the electrostatic screening. Values of $E_{d0} \approx 103 \text{ meV}$ and $\alpha \approx 14 \times 10^{-5} \text{ meV cm}$ are estimated. However, at high concentrations the donor activation energy drops to zero, indicating the crossover to metallic (non-activated) conductivity. The position of this drop agrees reasonably well with the concentration ($1.4 \times 10^{17} \text{ cm}^{-3}$) determined from the hopping transport and $\sigma(0)$ (see dashed line in figure 7).

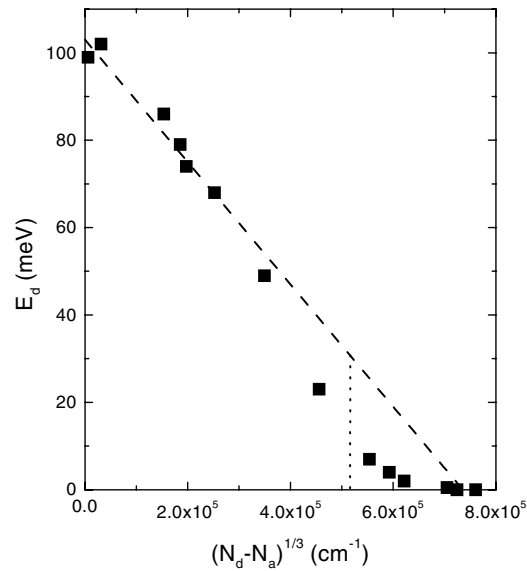


Figure 7. Thermal donor activation energy E_d as a function of the uncompensated, effective donor concentration $N_d - N_a$. The dashed line corresponds to a fit to equation (7) and the dotted line shows the critical donor concentration of the metal–insulator transition N_c .

Although the estimated value of the critical donor concentration in n-CGS corresponds reasonably well with the Mott criterion, one has to keep in mind that the introduced donor levels are not hydrogen-like. Assuming $m^* = 0.11 m_e$ and $\epsilon_r = 9.6$, an activation energy of 16 meV can be estimated for a hydrogen-like donor in n-CGS. This is much smaller than the value of 103 meV obtained for E_{d0} . Furthermore, the different samples show a different degree of compensation K ($K = N_a/N_d$). It has been reported that N_c for a given material also depends on compensation [32, 33]. However, the framework of the Anderson MIT accounts for a good qualitative description of the observed data and therefore, for the doping-induced MIT in compensated n-CGS.

4. Conclusions

The doping-induced Anderson-type metal–insulator transition in n-CuGaSe₂ single crystals is studied. A critical donor concentration of $1.4 \times 10^{17} \text{ cm}^{-3}$ is estimated, which is in good agreement with the Mott criterion. At low temperatures, variable range hopping is observed on the dielectric side of the transition. Furthermore, a crossover from Mott- to Efros–Shklovskii-type conduction is found. The maximum carrier concentration on the metallic side is limited by self-compensation due to intrinsic defects. A maximum donor concentration of $4.4 \times 10^{17} \text{ cm}^{-3}$ is achieved.

Acknowledgments

We are grateful to N Fabre for Ge-ion implantation and H Riazi-Nejad for growth of crystals. Furthermore, we would like to thank B Batlogg for use of his equipment.

References

- [1] Saad M, Bucher E and Lux-Steiner M Ch 1996 *Appl. Phys.* A 62 181
- [2] Nadenau V, Hariskos D and Schock H W 1997 *Proc. 14th Eur. Photovoltaic Solar Energy Conf. (Barcelona)* (Bedford: Stephens) p 1250
- [3] Schön J H, Fabre N, Oestreich J, Schenker O, Riazhi-Nejad H, Klenk M, Arushanov E and Bucher E 1999 *Appl. Phys. Lett.* **75** 2969
- [4] Emelyanenko O V, Lagunova T S and Nasledov D N, 1961 *Fiz. Tverd. Tela* **3** 198 (Engl. transl. 1961 *Sov. Phys. Solid State* **3** 144)
- [5] Mott N F 1967 *Adv. Phys.* **16** 49
- [6] Rincon C, Wasim S M and Ochoa J L 1995 *Phys. Status Solidi a* **148** 251
- [7] Anderson P W 1958 *Phys. Rev.* **102** 1008
- [8] Rosenbaum T F, Milligan R F, Paalanen M A, Thomas G A, Bhatt R N and Lin W 1983 *Phys. Rev. B* **27** 7509
- [9] Mott N F 1972 *Phil. Mag.* **26** 1015
- [10] Imry Y 1980 *Phys. Rev. Lett.* **44** 469
- [11] Klein A and Jaegermann W 1999 *Appl. Phys. Lett.* **74** 2283
- [12] Wei S H, Zhang S B and Zunger A 1998 *Appl. Phys. Lett.* **72** 3199
- [13] Zunger A, Zhang S B and Wei S H 1997 *Proc. 14th Eur. Photovoltaic Solar Energy Conf. (Barcelona)* (Bedford: Stephens) p 32
- [14] Schön J H 2000 *J. Phys. D: Appl. Phys.* at press
- [15] Kasiyan V A, Nedeoglo D D, Simashkevich A V and Timchenko I N 1989 *Phys. Status Solidi b* **154** 287
- [16] Mott N F 1968 *J. Non-Cryst. Solids* **1** 1
- [17] Shklovskii B I and Efros A L 1984 *Electronic Properties of Doped Semiconductors (Springer Series Solid State Science 45)* ed M Cardona (Berlin: Springer)
- [18] Rosenbaum R 1991 *Phys. Rev. B* **44** 3599
- [19] Lisunov S G, Arushanov E, Thomas G A, Bucher E and Schön J H 2000 *J. Appl. Phys.* submitted
- [20] Zhang Y, Dai P, Levy M and Sarachik M P 1990 *Phys. Rev. Lett.* **64** 2687
- [21] Roy A, Levy M, Guo X M and Sarachik P M 1989 *Phys. Rev. B* **39** 10 185
- [22] Schön J H 1998 *PhD Thesis* University of Konstanz
- [23] Marquez R and Rincon C 1995 *Phys. Status Solidi B* **191** 115
- [24] Thomas G A, Ootuka Y, Katsumoto S, Kobayashi S and Sasaki W 1982 *Phys. Rev. B* **25** 4288
- [25] Altshuler B L, Aronov A G and Lee P A 1980 *Phys. Rev. Lett.* **44** 1288
- [26] Abrahams E, Anderson P W, Licciardello D C and Ramakrishnan T V 1979 *Phys. Rev. Lett.* **42** 673
- [27] Matsubara T and Toyozawa Y 1961 *Prog. Theor. Phys.* **26** 739
- [28] Alexander M N and Holcomb D F 1968 *Rev. Mod. Phys.* **40** 815
- [29] Lee P A and Ramakrishnan T V 1982 *Phys. Rev. B* **26** 4009
- [30] Kawabata A 1980 *Solid State Commun.* **34** 431
- [31] Pearson G L and Bardeen J 1949 *Phys. Rev.* **75** 865
- [32] Zabrodskii A G 1980 *Sov. Phys.-Semicond.* **14** 886
- [33] Thomaschefskey U and Holcomb D F *Phys. Rev. B* **45** 13 356